Rare Metal Materials and Engineering
Volume 53, Issue 4, April 2024
Available online at www.rmme.ac.cn

Science Press

Cite this article as: Lan Xinyue, Wang Ping, Gong Zeyu, et al. Effect of Phytic Acid Modification on Characteristics of MAO Coating on TC4 Titanium Alloy[J]. Rare Metal Materials and Engineering, 2024, 53(04): 954-962. DOI: 10.12442/j.issn.1002-185X.20230376.

ARTICLE

Effect of Phytic Acid Modification on Characteristics of MAO Coating on TC4 Titanium Alloy

Lan Xinyue[1,2], Wang Ping[1,2], Gong Zeyu[1,2], Luo Xu[1], Zheng Youping[1], Deng Bowen[3]

[1] State Key Laboratory of Vanadium and Titanium Resources Comprehensive Utilization, Panzhihua 617000, China; [2] School of New Engineering and Materials, Southwest Petroleum University, Chengdu 610500, China; [3] Institute of Chemistry, Chinese Academy of Sciences, University of Chinese Academy of Sciences, Beijing 100190, China

Abstract: Phytic acid, one kind of organic acid, was added into the electrolyte to enhance the corrosion performance and thermal stability of micro-arc oxidation (MAO) coating on TC4 titanium alloy. The effect of phytic acid on the coating formation, morphology, and performance was analyzed by scanning electron microscope, X-ray diffractometer, X-ray photoelectron spectroscope, and thermal shock experiments. Results show that the addition of phytic acid leads to the refinement of discharge microholes and improves the formation efficiency and phase structure of MAO coating. Through potentiodynamic polarization tests, it is found that adding phytic acid can significantly enhance the corrosion resistance of MAO coating. The corrosion current density decreases from 8.406×10^{-5} A·cm^{-2} to 2.580×10^{-6} A·cm^{-2} when the phytic acid concentration in electrolyte changes to 12 mL/L (optimal phytic acid concentration). Cyclic high temperature oxidation test results indicate that the thermal shock resistance and high temperature oxidation resistance of TC4 alloy are enhanced.

Key words: TC4 titanium alloy; MAO; corrosion resistance; thermal shock resistance

TC4 titanium alloys have low density, excellent corrosion resistance, good heat resistance, and fine biocompatibility. They have extensive applications in the petrochemical, aerospace, and biomaterial[1–5]. In practical applications, titanium alloy has poor high temperature oxidation resistance and inferior thermal shock resistance, so it peels off easily because of the non-uniform oxidation at high temperature caused by rotational friction[6–8]. To mitigate this issue, titanium alloy needs surface protection before application. Common surface modification techniques are complicated, such as gas phase deposition, ion implantation, and laser cladding[9–11]. Micro-arc oxidation (MAO) is an environmental-friendly surface modification technique, attracting widespread attention for its easy production of corrosion-resistant ceramic coatings based on substrate oxides on the nonferrous metal surface, like magnesium, aluminum, and titanium[12–14].

However, MAO coatings often suffer from loose and porous surface due to the presence of discharge microholes and some small cracks, which adversely affect the corrosion resistance. To solve these problems, MAO coatings have been modified by introducing various substances into the electrolyte, which reduce the size of discharge micropores, increase the coating thickness, and reduce the porosity, thereby enhancing the overall quality and durability of MAO coatings. Chang et al[15] inhibited the formation of surface cracks of MAO coating on TC4 titanium alloy by adding SiC nanoparticles into electrolyte. Wang et al[16] studied the effect of $NaAlO_2$ content in the silicate electrolyte system on the ceramic MAO coating of pure titanium, and found that 0.2 g/L $NaAlO_2$ can improve the corrosion resistance of MAO coating. Zhong et al[17] applied $TiO_2/ZrO_2/Al_2TiO_5$ composite ceramic coating onto TC4 titanium alloy and revealed that the three-dimension porous network structure of MAO coating forms the metallurgical bonding interface between MAO coating and TC4 titanium alloy, thereby improving the thermal shock resistance of TC4 titanium alloy. Jiang et al[18]

Received date: June 13, 2023
Foundation item: Open Fund of State Key Laboratory of Vanadium and Titanium Resources Comprehensive Utilization (2022P4FZG08A); Sichuan Science and Technology Program (2022YFSY0018)
Corresponding author: Wang Ping, Ph. D., Professor, School of New Engineering and Materials, Southwest Petroleum University, Chengdu 610500, P. R. China, E-mail: 200731010041@swpu.edu.cn

employed MAO technique to prepare in-situ Ce^{3+} semiconductor coupled with TiO_2 photocatalytic coatings on TC4 titanium alloy, which significantly improved the photocatalytic performance of TiO_2 coatings. By adding a trace amount of rare earth compound $Ce(NO_3)_2$ into the electrolyte, Lan et al[19] reduced the number and size of pores in MAO coating and promoted the formation of stable corrosion-resistant rutile phase TiO_2 and CeO_2 in MAO reaction, leading to the enhancement in corrosion resistance of MAO coating. However, the addition of ceramic particles may cause uneven particle dispersion, difficult doping modification control, environment pollution caused by metal ions of some inorganic salts, and high manufacture cost due to the use of rare earth and rare earth oxides. The overall performance of MAO coatings should be further improved, particularly in the aspect of environmental-friendly additives.

In the design of MAO coatings, organic acids are valuable additives for the improvement of coating properties. It is reported that the addition of organic acids can affect the processing, improve the morphology, and alter the phase ratios, thus enhancing the MAO coating properties. Because most organic acids have electron-absorbing groups, the electrolyte stability can be improved by inhibiting the spark discharge behavior in MAO reaction. Then, the uniformity and compactness of MAO coating can be ameliorated[20–22]. Wei et al[22] eliminated the penetrating pores in the ultrasonic MAO coating on pure magnesium by adding phytic acid (PA, $C_6H_6(PO_4)_6H_{12}$), thereby improving the corrosion resistance. Pak et al[23] found that the mechanism of organic acid modification of MAO coating is mainly related to the cooperation of PA and magnesium ions. Zeng et al[24] found that the strong complexation of PA can be used to introduce metal ions into the reaction solution to greatly improve the corrosion resistance of PA chemical conversion coating on NZ30K magnesium alloy. Zhang et al[25] found that adding PA can decrease the porosity of MAO coating and increase the coating thickness.

However, the effect of PA addition on the properties of MAO ceramic coatings on TC4 titanium alloy is rarely reported. The structural formula of PA is shown in Fig. 1[26]. Because PA can easily ionize in aqueous solution, it has strong chelating ability with metal ions. In this case, O atoms of each phosphate group in PA can act as coordination atoms to complex with metal ions in pores, and then the chemical adsorption occurs in ceramic coatings and micropores.

In this research, the effect of PA concentration on MAO coating of TC4 titanium alloy was investigated. The coating formation process, morphology, corrosion resistance, thermal shock resistance, and high temperature oxidation resistance of MAO coating prepared by electrolyte containing PA with different concentrations were analyzed. Additionally, the mechanism of coating formation was discussed.

1 Experiment

The element composition of TC4 titanium alloy used in this research was V (3.5wt%–4.5wt%), Al (5.5wt%–6.8wt%), Fe

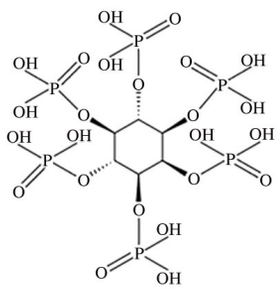

Fig.1 Structural formula of PA[26]

(≤0.3wt%), N (≤0.2wt%), O (≤0.2wt%), C (≤0.1wt%), H (≤0.5wt%), and titanium. The alloy plate was cut into specimens with 15 mm×15 mm×3 mm in size. Before MAO treatment, the specimens were polished by sandpapers (400#, 800#, 1200#) to eliminate the oxide layer. Then, the polished specimens were soaked in acetone solution for 2–3 min to remove oil, then rinsed by deionized water, and dried.

MAO treatment was conducted on TC4 titanium alloy by constant current MAO equipment (WDL20-6), which consisted of power source, treatment bath, cooling system, stirrer, and voltage monitoring system. The settings for MAO experiment were as follows: duty ratio of 80%, pulse frequency of 500 Hz, current density of 7 $A \cdot dm^{-2}$, and oxidation time of 45 min. The sodium silicate and sodium phosphate mixed solutions were served as the base electrolyte. PA with different concentrations (0, 3, 6, 9, 12 $mL \cdot L^{-1}$) was added into the base electrolyte. During MAO process, the specimen was used as the anode and the stainless-steel sheet was used as the cathode. The electrolyte was continuously stirred throughout MAO process to ensure the uniform particle dispersion. The electrolyte temperature was fixed at approximately 35 °C by continuous mechanical stirring. After MAO treatment, the specimen was immersed in deionized water at 90 °C for 5 min.

Scanning electron microscope (SEM, ZEISS EVO MA15) was used to characterize the surface appearance and cross-sectional morphologies of MAO coating. The distribution of Ti, C, O, P, and Si elements on MAO coating surface was investigated by energy dispersive spectroscope (EDS, OXFORD 20). X-ray diffraction (XRD, DX-2700B) analysis was conducted to determine the phase composition of MAO coating. The scanning angle (2θ) range was set from 10° to 80° and the scanning rate was $0.05° \cdot s^{-1}$. X-ray photoelectron spectroscope (XPS, XSAM-800) was used to determine the chemical bonding and oxidation states of atoms in surface compounds. The microhardness was measured by microhardness meter (HVS-1000) at 1.96 N for 15 s. Thermal shock resistance of MAO coating was tested by the muffle furnace (SX-G12123). Before tests, the specimens were rinsed by acetone and ultrasonically cleaned by deionized water. The specimens were held at 400 °C for 5 min in muffle furnace (SX-G12123), cooled in deionized water, and then sent back to the muffle furnace for the next thermal cycle. This process

was repeated for 50 times. As for the tests of high temperature oxidation resistance, the specimens were held at 800 °C for 10 h and then cooled to room temperature. This process was repeated for 10 times. The specimen mass before and after each high temperature oxidation cycle was measured.

The corrosion resistance of MAO coating under specific conditions was evaluated through potentiodynamic polarization curve measurements, which were conducted by electrochemical workstation (Gamry Reference 3000, USA). Before tests, the specimens were thoroughly rinsed by acetone and subsequently immersed in ethanol with ultrasonic stirring for 10 min. Afterwards, the specimens were rinsed by deionized water and dried under ambient conditions. The specimen was used as the working electrode. The saturated mercury chloride electrode was used as the reference electrode, and the platinum electrode was used as the counter electrode. The specimen was then placed in 3.5wt% NaCl solution with exposed area of 2.25 cm^2. The temperature of corrosion solution was 20 ° C, the conductivity was 53 $mS \cdot cm^{-1}$, and the pH value of solution was 6.8. The ambient temperature was fixed at 25 °C. The potentiodynamic polarization curve measurements were initiated at − 250 mV. The potential scanning rate was 0.5 $mV \cdot s^{-1}$ and the final potential was 250 mV. Before polarization, the specimens were immersed for 600 s.

2 Results and Discussion

2.1 Influence of PA concentration on oxidation voltage

As shown in Fig. 2, without PA addition, the oxidation voltage exhibits a sharp increase during the initial anodic oxidation stage. After reaction for 1 min, the oxidation voltage increases swiftly, reaching approximately 200 V. At this stage, the spark is too weak to be observed[27]. After 3 min, the voltage increasing rate gradually declines from 1.2 $V \cdot s^{-1}$ to 0.5 $V \cdot s^{-1}$, inferring the onset of spark stage for oxidation. After 5 min, MAO stage begins, and the voltage increasing rate moderately increases from 0.2 $V \cdot s^{-1}$ to 0.3 $V \cdot s^{-1}$. The number of discharge sparks occurring on the coating surface decreases, whereas the size of sparks gradually increases[28]. The voltage is increased obviously with increasing the PA concentration. The voltage reaches 517 V when PA concentration is 12 $mL \cdot L^{-1}$. Briefly, the duration and intensity of both the ordinary anodic oxidation and anodic spark oxidation stages gradually increase, but the breakdown voltage decreases. The decrement is in proportion to the PA concentration.

2.2 Morphology and element distribution of MAO coating

According to Fig. 3a – 3e, the surfaces of MAO coatings have discernible changes with increasing the PA concentration. Without PA addition, numerous irregular micropores and microcracks appear on the coating surface, which is attributed to the increase in internal stress caused by incomplete thermal relaxation[26]. When PA concentration increases from 3 $mL \cdot L^{-1}$ to 12 $mL \cdot L^{-1}$ (Fig. 3b – 3e), the number and size of micropores on the coating surface decrease, and the pores have more uniform distribution. Because the molten metals and oxides are caused by the sparks with high energy, the scattered protrusions and melts are increased, the microcracks are decreased, and the coating becomes more compact. Besides, most micropores are blocked by the molten metals and oxides[29].

The contents of surface element of MAO coating on TC4 titanium alloy were analyzed by EDS, and the results are listed in Table 1. It can be seen that C and P elements are incorporated into the MAO coatings after adding PA into the electrolytes. When PA concentration increases from 0 $mL \cdot L^{-1}$ to 12 $mL \cdot L^{-1}$, the contents of C and P elements increase rapidly by a factor of 1.45 and 2, respectively. When PA concentration reaches 12 $mL \cdot L^{-1}$, the contents of C and P elements reach the maximum values as 11.13at% and 12.04at%, respectively. With increasing the PA concentration, the O element content is changed slightly, and the Ti content is decreased by 50% and then increased.

Fig. 4 presents the cross-sectional morphologies of MAO coatings prepared by electrolyte containing PA of different concentrations. It can be seen that there is no obvious dividing line between the external porous layer and the inner dense layer. Furthermore, the coating thickness is increased from 11 μm to 25 μm with increasing the PA concentration. When the PA concentration is 12 $mL \cdot L^{-1}$, partial outermost MAO coating exfoliates. This is because PA complex of the outermost layer is more sufficiently chelated with the metal ions, reducing the binding bond. Additionally, the hydrogen bonds of the outermost layer are weaker than those of the

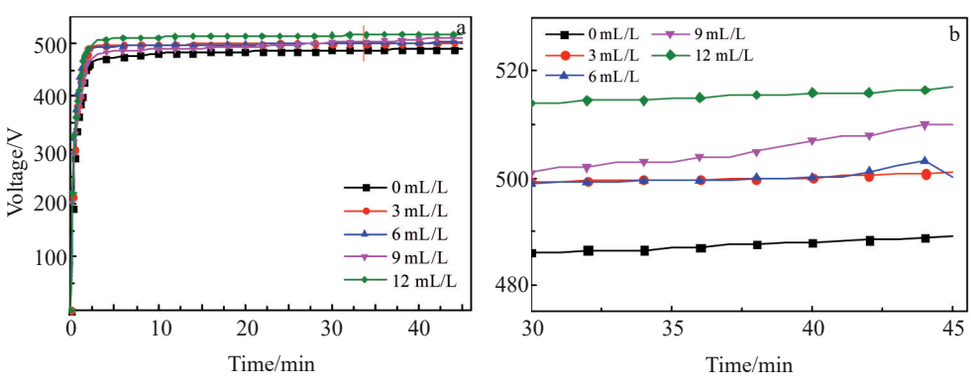

Fig.2 Overall (a) and magnified (b) images of influence of PA concentration on oxidation voltage

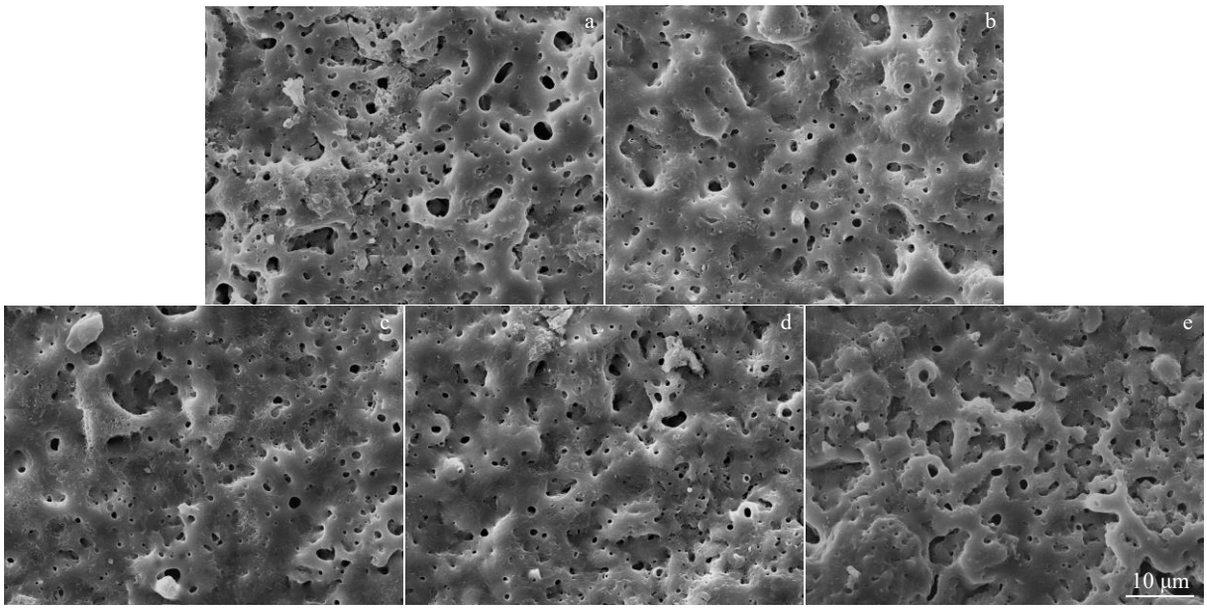

Fig.3 Surface morphologies of MAO coatings prepared by electrolyte containing PA of different concentrations: (a) 0 mL/L, (b) 3 mL/L, (c) 6 mL/L, (d) 9 mL/L, and (e) 12 mL/L

inner layer. Therefore, the binding force of the outermost layer is weak, which easily leads to crack and even exfoliation of MAO coating[27]. Briefly, with increasing the PA concentration, the chelate generated by PA and substrate increases the oxidation voltage. At the same time, the size and number of discharged micropores decrease.

2.3 Phase composition of MAO coating surface

Fig. 5 shows XRD patterns of MAO coatings prepared by electrolyte containing PA of different concentrations. It can be seen that MAO coatings are primarily composed of Ti, and they contain a small amount of Al_2TiO_5, α-Al_2O_3, SiO_2,

Table 1 Effects of PA concentration on surface element contents of MAO coating on TC4 titanium alloy (at%)

Element	PA concentration/mL·L^{-1}				
	0	3	6	9	12
Ti	32.33	27.93	18.60	15.59	33.35
C	6.28	10.77	11.29	9.45	11.13
O	42.09	37.06	42.17	42.47	34.23
P	4.90	6.11	6.29	8.59	12.04
Si	14.40	18.11	21.65	23.90	9.25

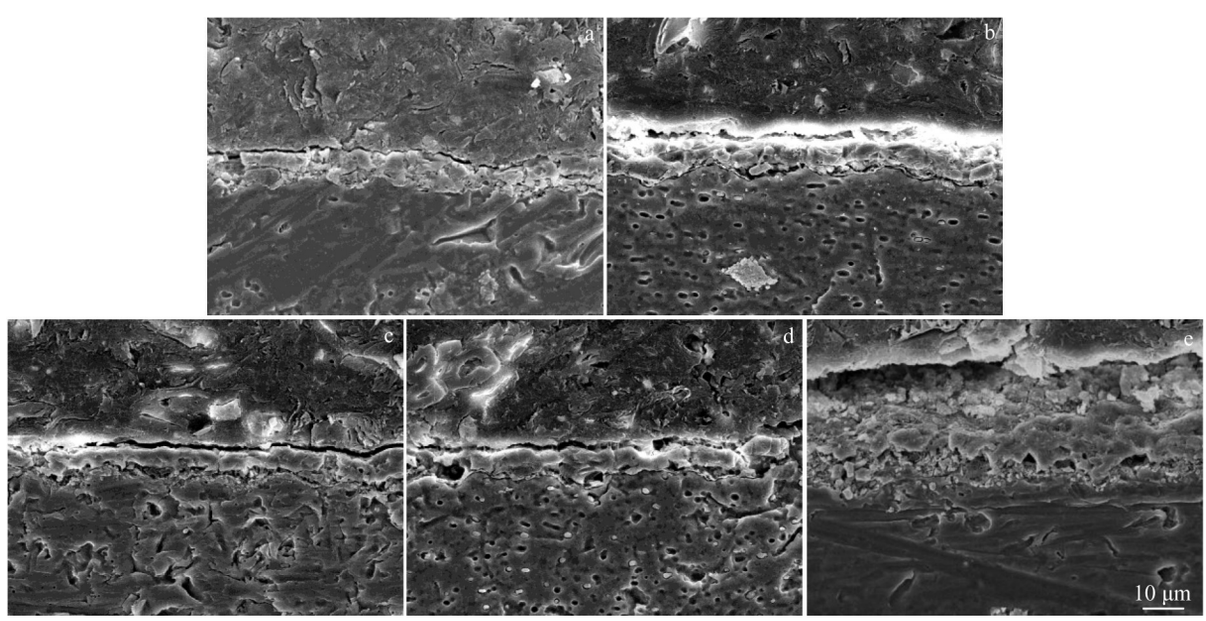

Fig.4 Cross-sectional morphologies of MAO coatings prepared by electrolyte containing PA of different concentrations: (a) 0 mL/L, (b) 3 mL/L, (c) 6 mL/L, (d) 9 mL/L, and (e) 12 mL/L

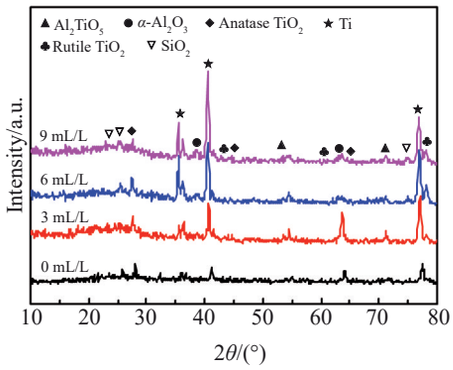

Fig.5 XRD patterns of MAO coatings prepared by electrolyte containing PA of different concentrations

rutile TiO_2, and anatase TiO_2. When PA concentration increases from 0 mL·L^{-1} to 12 mL·L^{-1}, the peak intensity of Ti in MAO coatings slowly decreases, whereas the peak intensities of anatase and rutile TiO_2 gradually increase. Adding PA in the preparation process of MAO coating can promote the crystal transformation, and the phase composition of MAO coatings is changed slightly with increasing the PA concentration.

Fig. 6 shows Raman spectra of MAO coatings prepared by electrolyte containing PA of different concentrations. It is obvious that the peaks at 767, 834, 1403, and 1572 cm^{-1} correspond to scissors mode of C_6-C_5-C_4, stretching vibration

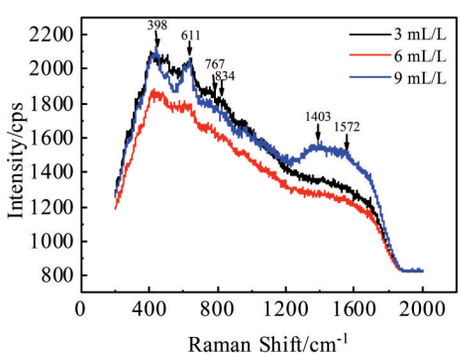

Fig.6 Raman spectra of MAO coatings prepared by electrolyte containing PA of different concentrations

of O_8-P_{14}=O_{23}, antisymmetric stretching vibration of C_1-O_8-P_{14}, and asymmetry hexatomic ring, respectively. This result is consistent with the surface-enhanced Raman scattering vibration peaks of PA molecule. Anatase is characterized by 15 optical modes with normal vibrations: $A_{1g}(R)+2B_{1g}(R)+3E_g(R)+B_{2u}(ia)+A_{2u}(IR)+2E_u(IR)$ [30]. Among them, six atomic vibrations, including $1A_{1g}(R)$, $2(B_{1g})$, and $3E_g(R)$ are Raman-active[31]. The Raman shift at 398 cm^{-1} exhibits the highest intensity among the observed peaks. Furthermore, the anatase exhibits 11 optical modes for the normal vibrations, including $A_{1g}(R)$, $A_{2g}(ia)$, $B_{1g}(R)$, $B_{2g}(R)$, $E_g(R)$, $A_{2u}(IR)$, $2B_{1l}(ia)$, and $3E_u(IR)$. The Raman shift at 611 cm^{-1} is related to A_{1g} rutile peaks.

Fig. 7 shows XPS spectra obtained from MAO coatings prepared by electrolyte containing PA of different concentrations. When the PA concentration increases from 3 mL·L^{-1} to 12 mL·L^{-1}, the binding energy of approximately 133 eV can be observed, corresponding to P 2p in Na_2PHO_4 and PHO_4^{2-} which has regular tetrahedral space structure (Fig. 7b). This result is consistent with the O-P=O structure obtained by Raman spectrum in Fig. 6. According to XPS analysis, the P element content is 0.82at%.

2.4 Hardness of MAO coating

Fig. 8 shows the microhardness of MAO coatings prepared by electrolyte containing PA of different concentrations. It can be seen that the microhardness is firstly increased and then decreased slightly with increasing the PA concentration. Without PA addition, the microhardness reaches 4621.7 MPa. With increasing the PA concentration, the microhardness is increased gradually. When the PA concentration is 2 mL·L^{-1}, the micro-penetration hardness increases to 5217.5 MPa, indicating that the microhardness increases significantly after adding PA. Excess PA addition barely has influence on the microhardness of MAO coating.

2.5 Effect of PA concentration on corrosion resistance of MAO coating

Fig. 9 shows the electrochemical properties of MAO coatings prepared by electrolyte containing PA of different concentrations, which are reflected by the zeta potential polarization curves. Table 2 shows the corrosion velocity corresponding to the polarization curve. V_{corr} is corrosion rate (mm·a^{-1}), I_{corr} is the self-corrosion current density (A·cm^{-2}),

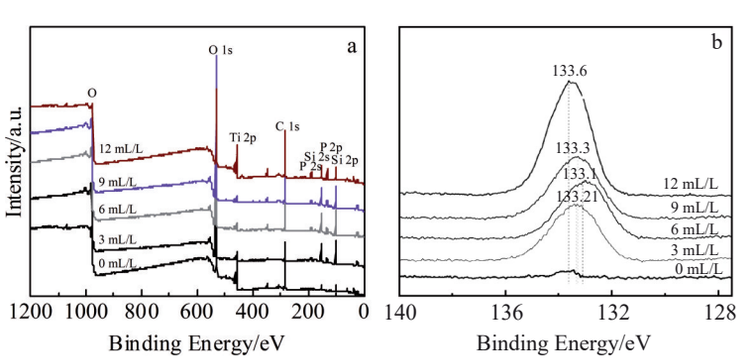

Fig.7 XPS spectra of MAO coatings prepared by electrolyte containing PA of different concentrations: (a) overall and (b) P 2p

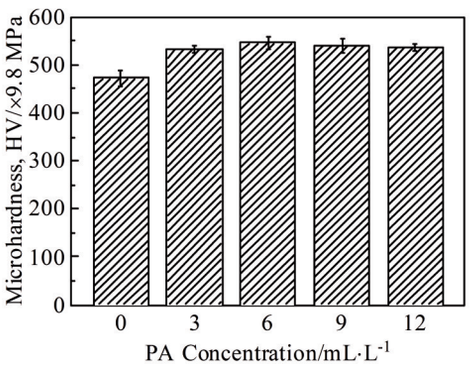

Fig.8 Micohardness of MAO coatings prepared by electrolyte containing PA of different concentrations

and E_{corr} is the self-corrosion potential (V) of the coatings[30]. E-lg$i$ data are governed by the kinetics shown in Fig. 9. The calculation equations are as follows:

$$I_{corr} = \beta_a\beta_c/[(\beta_a + \beta_c)R_p] \quad (1)$$

$$V_{corr} = \frac{I_{corr} \times N \times 393.7}{\rho \times 365 \times 24 \times 3600} \div 96500 \div 39.37 \quad (2)$$

where β_a and β_c are the anodic and cathodic Tafel parameters obtained by the slopes of polarization curves ($\partial E_{corr}/\partial \lg I_{corr}$), respectively; R_p is the polarization resistance ($\Omega \cdot cm^2$) obtained by $\partial E/\partial \lg i$ (E is the potential and i is the current density) at time $t=\infty$ and $\Delta E=0$[30]; ρ is density ($g \cdot cm^{-3}$); N is the sample mass[30].

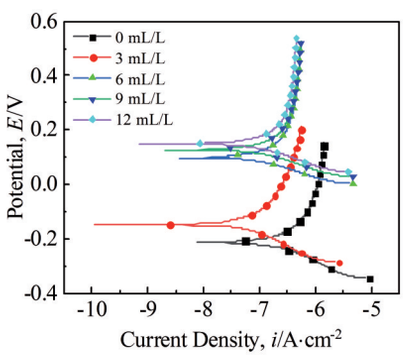

Fig.9 Polarization curves of MAO coatings prepared by electrolyte containing PA of different concentrations

With increasing the PA concentration from 0 mL·L^{-1} to 12 mL·L^{-1}, the corrosion current density is decreased by 53%, whereas the corrosion potential is increased by 0.35 V towards the positive side. These results indicate that the PA addition decreases the corrosion rate of MAO coating. When PA concentration reaches 12 mL·L^{-1}, the highest corrosion potential (0.143 V) is obtained, the minimum corrosion current density (2.580×10^{-6} A·cm^{-2}) is achieved, and corrosion velocity is the lowest (8.5916×10^{-3} mm·a^{-1}). Therefore, the PA addition enhances the corrosion resistance of MAO coating, and the optimal corrosion resistance can be achieved when PA concentration is 12 mL·L^{-1}. This is mainly because the quantity and dimension of the micropores on the coating surface greatly decrease, compared with those without PA addition, which is also confirmed by SEM images in Fig.3.

2.6 Effect of PA concentration on thermal shock resistance and high temperature oxidation resistance of MAO coating

Fig. 10 shows surface morphologies of MAO coatings prepared by electrolyte containing PA of different concentrations after thermal shock cycles. After heat treatment, the binding interface shows a concave-convex structure, and a small number of microcracks appear on the external coating. It is evident that the number and size of micropores on the coating are decreased with increasing the PA concentration, as shown in Fig.10b–10e. It can be seen that MAO coating bonds well with the substrate, because of the special multilayer structure of MAO coating, which is composed of loose and dense layers, therefore reducing the damage of thermal stress.

Fig.11 shows the mass gain rate of MAO coatings prepared by electrolyte containing PA of different concentrations after high temperature oxidation cycles at 800 °C. The mass gain rate of metal oxide coating is characterized by ΔW ($\Delta W=\Delta m/S$, where Δm is the mass difference and S is the unit area). Oxidation kinetics curve can be obtained by the time dependence of ΔW. The oxidation process roughly conforms to the parabola law, which indicates that the coating is compact and has resistance against high temperature oxidation.

Table 3 shows the mass gain of MAO coatings prepared by

Table 2 Polarization curve results of MAO coatings prepared by electrolyte containing PA of different concentrations

PA concentration/mL·L^{-1}	Corrosion potential, E_{corr}/V	Corrosion current density, I_{corr}/A·cm^{-2}	Corrosion velocity, V_{corr}/mm·a^{-1}
0	−0.215	8.406×10^{-5}	1.8617×10^{-2}
3	−0.164	1.325×10^{-6}	4.4123×10^{-3}
6	0.097	2.640×10^{-6}	8.7914×10^{-3}
9	0.129	2.652×10^{-6}	8.8313×10^{-3}
12	0.143	2.580×10^{-6}	8.5916×10^{-3}

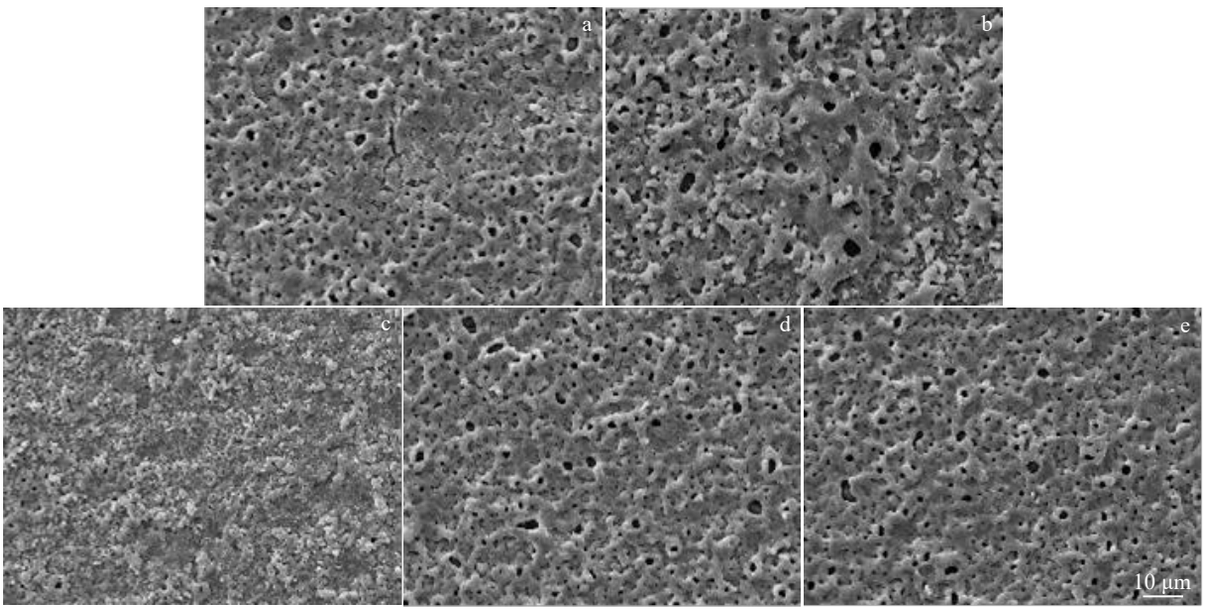

Fig.10 Surface morphologies of MAO coatings prepared by electrolyte containing PA of different concentrations after thermal shock cycles: (a) 0 mL/L, (b) 3 mL/L, (c) 6 mL/L, (d) 9 mL/L, and (e) 12 mL/L

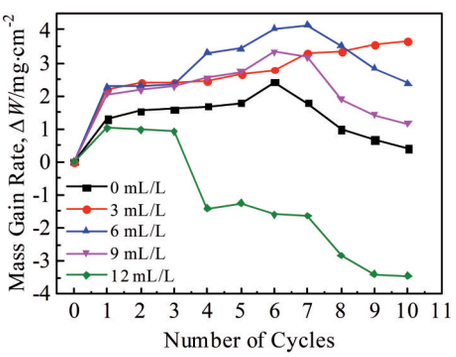

Fig.11 Mass gain rate (ΔW) curves of MAO coatings prepared by electrolyte containing PA of different concentrations after high temperature oxidation cycles at 800 °C

electrolyte containing PA of different concentrations after high temperature oxidation cycles at 800 °C. Without PA addition, the specimen mass is increased with the oxidation process proceeding. According to Fig. 11, the curve shows an inflection point at the 6th high temperature oxidation cycle. After that, the mass gain decreases. After 10 cycles of high temperature oxidation, the oxidation kinetics curves become irregular, but also roughly in accord with the parabolic law, which indicates that MAO coating has good cyclic oxidation resistance. This is because without PA addition, the coating is mainly composed of TiO_2 and Al_2O_3. According to the principle of Pilling Bedworth (P-B), the P-B ratios of TiO_2 and Al_2O_3 are greater than 1, which are 1.95 and 1.28[31], respectively. Therefore, the coating structure is compact, presenting protective effect. With increasing the PA concentration, ΔW is increased firstly and then decreased. When the PA concentration is 3 mL·L^{-1}, ΔW continues to increase during the high temperature oxidation process, and the ΔW value after 10 cycles of high temperature oxidation is the largest, which increases by 3.65 mg·cm^{-2}. These results suggest that the optimal high temperature oxidation resistance

Table 3 Mass gain of MAO coatings prepared by electrolyte containing PA of different concentrations after high temperature oxidation cycles at 800 °C (g)

PA concentration/mL·L^{-1}	High temperature oxidation cycle										
	0	1	2	3	4	5	6	7	8	9	10
0	3.0189	3.0271	3.0286	3.0289	3.0295	3.0302	3.0341	3.0302	3.0251	3.0231	3.0215
3	2.9934	3.0072	3.0084	3.0085	3.0089	3.0101	3.0110	3.0125	3.0127	3.0141	3.0148
6	2.9526	2.9669	2.9671	2.9675	2.9734	2.9742	2.9780	2.9787	2.9747	2.9705	2.9676
9	3.0186	3.0315	3.0324	3.0329	3.0346	3.0358	3.0396	3.0386	3.0305	3.0276	3.0253
12	3.0375	3.0439	3.0436	3.0433	3.0286	3.0296	3.0274	3.0271	3.0196	3.0161	3.0158

of MAO coating can be achieved when PA concentration is 3 $mL \cdot L^{-1}$.

3 Conclusions

1) After PA addition, the final voltage firstly increases and subsequently decreases. Additionally, the duration and intensity of both the ordinary anodic oxidation and anodic spark oxidation stages gradually increase, but the breakdown voltage decreases. The decrement is in proportion to the PA concentration. Adding PA changes the morphology and structure of MAO coating and improves the formation, thereby increasing the coating thickness.

2) Adding PA in the preparation process of MAO coating can promote the crystal transformation. During MAO process, Ti is oxidized to TiO_2, and the coating mainly consists of α-Al_2O_3, Al_2TiO_5, SiO_2, rutile TiO_2, and anatase TiO_2. With increasing the PA concentration, the anatase content in the coating is increased.

3) With increasing the PA concentration, the chelate generated by PA and substrate increases the oxidation voltage. At the same time, the size and number of discharged micropores decrease, and the coating microhardness improves, which enhance the corrosion resistance and high temperature oxidation resistance of the TC4 titanium alloy.

4) When the PA concentration is 12 $mL \cdot L^{-1}$, the corrosion resistance of TC4 titanium alloy in 3.5wt% NaCl solution is optimal, the corrosion voltage is the largest of 0.143 V, and the self-corrosion current density reaches the smallest as 2.580×10^{-6} $A \cdot cm^{-2}$. When PA concentration is 3 $mL \cdot L^{-1}$, the coating exhibits optimal resistance against the thermal shock and high temperature oxidation.

References

1 Lu J W, Zhao Y Q, Niu H Z *et al. Materials Science and Engineering*[J], 2016, 62: 32

2 Shan D B, Yang G P, Xu W C. *Journal of Materials Processing Technology*[J], 2009, 209(17): 5713

3 Luo Lei, Duan Ximing, Yang Xirong *et al*. *Materials China*[J], 2022, 41(4): 314 (in Chinese)

4 Gao W, Liu J N, Ding Z S *et al*. *Rare Metal Materials and Engineering*[J], 2022, 51(5): 1537

5 Lü K, Zhang R F, Chen W D *et al*. *Rare Metal Materials and Engineering*[J], 2022, 51(11): 4103

6 Dai J J, Zhu J Y, Chen C Z *et al*. *Journal of Alloys and Compounds*[J], 2016, 685: 784

7 Ebach-Stahl A, Eilers C, Laska N *et al*. *Surface and Coatings Technology*[J], 2013, 223: 24

8 Lee D B, Habazaki H, Kawashima A *et al. Corrosion Science*[J], 2000, 42: 721

9 Zhang L C, Chen L Y, Wang L Q. *Advanced Engineering Materials*[J], 2019, 22: 1901258

10 Ji P F, Lü K, Chen W D *et al*. *Rare Metal Materials and Engineering*[J], 2023, 52(5): 1583

11 Wang X J, Wang P, Liu Y *et al*. *Rare Metal Materials and Engineering*[J], 2023, 52(10): 3452

12 Liu F C, Mao Y Q, Lin X *et al*. *Optics & Laser Technology*[J], 2016, 83: 140

13 Wang S Q, Wang Y M, Cao G *et al*. *Corrosion Science*[J], 2023, 216: 11076

14 Lu J L, Yin X J, Kuan A T L *et al*. *Electroplating & Finishing*[J], 2012, 9: 21

15 Chang Hai, Guo Xuegang, Wen Lei *et al*. *Journal of Materials Engineering*[J], 2019, 47(3): 109 (in Chinese)

16 Wang P, Wu T, Peng H *et al*. *Materials Letters*[J], 2016, 170: 171

17 Zhong Y S, Shi L P, Li M W *et al*. *Applied Surface Science*[J], 2014, 311: 158

18 Jiang X D, Wang Y Q, Pan C X. *Journal of Alloys and Compounds*[J], 2011, 509: 137

19 Lan X Y, Xiong D, Wang P *et al*. *Materials Science and Technology*[J], 2022, 38: 1585

20 Zhang R F, Qiao L P, Qu B *et al*. *Materials Letters*[J], 2015, 153: 77

21 Zhang R F, Zhang S F, Duo S W. *Applied Surface Science*[J], 2009, 255: 7893

22 Wei Fanghong, Li Muqin, Guo Xiaojuan *et al*. *China Surface Engineering*[J], 2015, 28(2): 78 (in Chinese)

23 Pak S, Jiang Z H, Yao Z P *et al*. *Surface and Coatings Technology*[J], 2017, 325: 579

24 Zeng Jiyong, Guo Xinwu, Guo Jiacheng *et al*. *Surface Technology*[J], 2019, 48(10): 230 (in Chinese)

25 Zhang Rongfa, Wang Fangyuan, Lou Jin *et al*. *Journal of Functional Materials*[J], 2007, 38(Supplement): 3762 (in Chinese)

26 Xu Y C, Guo Y T, Li G Y *et al*. *Progress in Organic Coatings*[J], 2022, 169: 106920

27 Yang B, Wang P, Hu J *et al*. *International Journal of Materials Research*[J], 2022, 113(8): 693

28 Wang P, Gong X, Li H L *et al*. *Surface Engineering*[J], 2019, 36: 216

29 Chen X W, Li M L, Zhang D F *et al*. *Surface and Coatings Technology*[J], 2022, 433: 128127

30 Scully J R. *Corrosion*[J], 2000, 56(2): 199

31 Siony N, Vuong L, Lundaajamts O *et al*. *Materials Today Communications*[J], 2022, 33: 104465

植酸修饰改性对TC4钛合金微弧氧化膜层性能的影响

兰欣悦[1,2]，王　平[1,2]，龚泽宇[1,2]，罗　许[1]，郑友平[1]，邓博文[3]

(1. 钒钛资源综合利用国家重点实验室，四川 攀枝花 607000)

(2. 西南石油大学 新能源与材料学院，四川 成都 610500)

(3. 中国科学院大学 中国科学院化学研究所，北京 100190)

摘　要：通过向电解液中添加有机酸植酸，提升了TC4钛合金微弧氧化涂层的耐腐蚀性能和热稳定性。通过扫描电子显微镜、X射线衍射仪、X射线光电子能谱仪和热冲击实验等技术手段，分析了植酸对涂层形成、形貌和性能的影响。结果显示，植酸的添加使放电微孔更加细小，提高了涂层的形成效率并优化了相结构。通过动电位极化测试，发现添加植酸显著提高了微弧氧化涂层的耐腐蚀性能。将电解液中的植酸浓度调整为12 mL/L（最佳植酸浓度）后，腐蚀电流密度由8.406×10^{-5} A·cm^{-2}降低至2.580×10^{-6} A·cm^{-2}。循环高温氧化试验结果表明，TC4钛合金的耐热冲击性能和高温抗氧化性能得到了改善。

关键词：TC4钛合金；微弧氧化；耐腐蚀性能；耐热冲击性能

作者简介：兰欣悦，女，1997年生，硕士生，西南石油大学新能源与材料学院，四川 成都 610500，E-mail：345125965@qq.com